J|A|C|S
COMMUNICATIONS

Published on Web 04/03/2007

Morphology Control of Fluorescent Nanoaggregates by Co-Self-Assembly of Wedge- and Dumbbell-Shaped Amphiphilic Perylene Bisimides

Xin Zhang, Zhijian Chen, and Frank Würthner*

Universität Würzburg, Institut für Organische Chemie and Röntgen Research Center for Complex Material Systems, Am Hubland, D-97074 Würzburg, Germany.

Received February 12, 2007; E-mail: wuerthner@chemie.uni-wuerzburg.de

Perylene bisimides (PBIs) have been extensively studied as building blocks for functional supramolecular architectures in nonpolar solvents through hydrogen bonding, metal ion coordination, and $\pi-\pi$ stacking interaction.[1] In contrast, little attention was paid to the self-assembly behavior of PBIs in aqueous solution.[2] Amphiphilic molecules, consisting of hydrophobic and hydrophilic moieties, self-assemble into highly organized aggregates with various morphologies such as spherical micelles, wormlike micelles, spherical and hollow vesicles, planar bilayers, nanotubes, and others.[3] The formation of these morphologies depends on solvent environments, molecular structures and shapes, as well as the relative fraction of hydrophilic and hydrophobic parts.[4] On the other hand, the stabilization of self-assembled superstructures through covalent linkage, for example, by polymerization, is of great interest for the practical application of supramolecular chemistry.[5] By covalent stabilization, the aggregate dimension and shape can be captured, and aggregate strength can be increased.[6] Here, we report for the first time that the nanoaggregates of perylene bisimides with particular morphology can be obtained by self-assembly of differently shaped amphiphilic PBIs in aqueous solution.

Chart 1

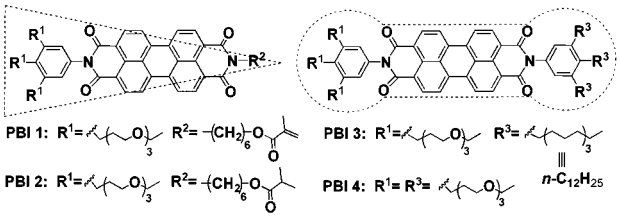

In this work, the wedge- and dumbbell-shaped amphiphilic perylene bisimides PBI **1**−**4** (Chart 1) were synthesized and fully characterized (see details in Supporting Information). The absorption and fluorescence spectra of molecularly dissolved PBI **1**−**4** display a mirror-image relationship with a small Stokes' shift (5−6 nm) in "good" solvents such as CH_2Cl_2 and THF (Figure S-15 in Supporting Information). Upon addition of the "bad" solvent water into the THF solution, a gradual decrease in fluorescence intensity at 500−600 nm was observed as exemplified for PBI **1** (Figure 1), and a new broad and structureless fluorescence band appears at 600−800 nm owing to excimer formation.[7] These observations imply that monomeric PBI **1** self-assembles into fluorescent multimolecular aggregates in aqueous solution.

For the wedge-shaped PBI **1**, Israelachvili's critical packing parameter (P_c)[8] was calculated to be 0.252, implying that spherical micelles should be favorably formed in polar solvents ($P_c < 1/3$ for micelle formation).[8a] The theoretical prediction was confirmed by transmission electron microscopic (TEM) studies. A large number of spherical micelles with the diameter of 4−6 nm were observed for PBI **1** in THF-containing water (2%, v/v) as shown in Figure 2a. The micelles were formed with a narrow polydispersity and a high degree of curvature due to the conical structure. The same aggregation behavior was also observed for PBI **2**. In contrast, dumbbell-shaped PBI **4** self-assembled into rod aggregates with a diameter of 4 nm (Figure 2b). The formation of well-defined aggregates of these PBIs may be attributed to the $\pi-\pi$ stacking interaction between the perylene cores along one-dimensional long axis without curvature, and stabilized by surrounding hydrophilic chains as shown in Scheme 1(bottom).

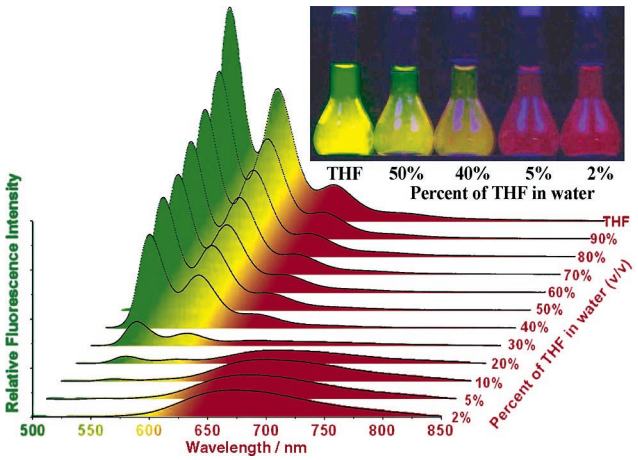

Figure 1. Fluorescence spectra of PBI **1** in THF and THF-containing water, $\lambda_{ex} = 490$ nm, [PBI **1**] $= 2 \times 10^{-6}$ M. The inset shows a photograph of PBI **1** in THF and THF-containing water under UV-light irradiation.

More interestingly, hollow vesicles were observed for the co-self-assembled system of PBI **1** and PBI **3** ([PBI **1**]/[PBI **3**] = 8/1 in molar ratio) in THF-containing water (2%, v/v) as shown in Figure 2c. Spherical vesicles were formed with the average diameter of 94 nm and the wall thickness of 7−8 nm, which is approximately twice the length of a single optimized molecule PBI **1** (3.3 nm) or PBI **3** (4.0 nm) in water. The aggregation number for the inner and outer layers were calculated to be approximate 2.9×10^5 and 3.2×10^5, respectively, from the bilayer volume divided by the volume of the single molecule. For the co-self-assembled system with higher PBI **3** content ([PBI **1**]/[PBI **3**]= 4/1), bilayer vesicles were observed with a larger average diameter of 133 nm in THF-containing water (2%, v/v) as shown in Figure 2e. The size distribution of these co-aggregates also became broader at higher PBI **3** content as measured from TEM (Figure 2g,h) and dynamic light scattering (DLS) (Figure S-24), and these large vesicles emit red fluorescence (Figure 2f).

The observed variation of the aggregates' shape and size can be rationalized by considering spontaneous curvature. When dumbbell-shaped PBI **3** is co-self-assembled with wedge-shaped PBI **1**, the average hydrophobic part increases, and the interface between the hydrophilic and hydrophobic parts changes from a curved interface to a more flat one. The resulting decrease in spontaneous curvature releases the strain in the initially formed micelles with a high curvature, leading to micelle growth and a transition to vesicles as

10.1021/ja070994u CCC: $37.00

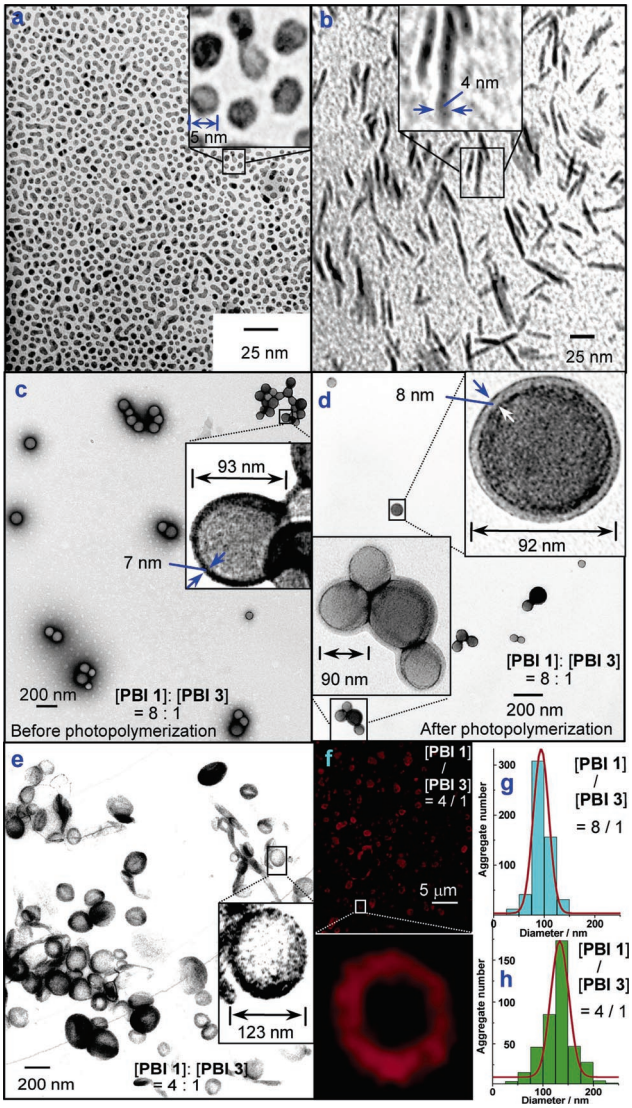

Figure 2. TEM images of self-assembled PBI **1** (a), PBI **4** (b), and before (c) and after (d) photopolymerization of co-aggregates of PBI **1** and PBI **3** in a 8:1 molar ratio; TEM (e) and confocal fluorescence images (f) of co-aggregates of PBI **1** and PBI **3** in a 4:1 molar ratio in THF-containing water (2%, v/v); and size distribution obtained from 548 co-aggregates ([PBI **1**]/[PBI **3**] = 8/1) (g), and from 402 co-aggregates ([PBI **1**]/[PBI **3**] = 4/1) (h). [PBI **1**] = 0.5 mg/mL (4.32×10^{-4} M); [PBI **4**] = 0.5 mg/mL.

illustrated in Scheme 1 (top and middle). It is interesting to note that such mechanism for the control of self-assembly by spontaneous curvature is present in biology. A typical example is the deformation of flat lipid membranes by protein coating into transport spherical vesicles.[9]

To stabilize these nanoaggregates, the in situ photopolymerization was performed in an organized state using 2,2-dimethoxy-2-phenylacetophenone as photoinitiator under UV irradiation at 350 nm. This wavelength was chosen because the photoinitiator has a maximum absorption at 350 nm, where perylene chromophores have a very weak absorption.[1] After photopolymerization, the vesicles from co-self-assembly retained their original shapes as shown in Figure 2d. The photopolymerization was confirmed by infrared (IR) studies. The vibration band at 968.1 cm^{-1} (characteristic vibration of $\delta(=CH_2)$ wagging mode) disappears after photopolymerization (Figure S-23). These vesicles do not change their morphology after the addition of PBI **3**, confirming that the vesicle structures are locked by photopolymerization.

Scheme 1. Schematic Illustration for the Formation of Micelles from Wedge-Shaped PBI **1** (top), Bilayer Vesicles from the Co-self-assembly of PBI **1** and Dumbbell-Shaped PBI **3** (middle), and Rod Aggregates from Dumbbell-Shaped PBI **4** (bottom).

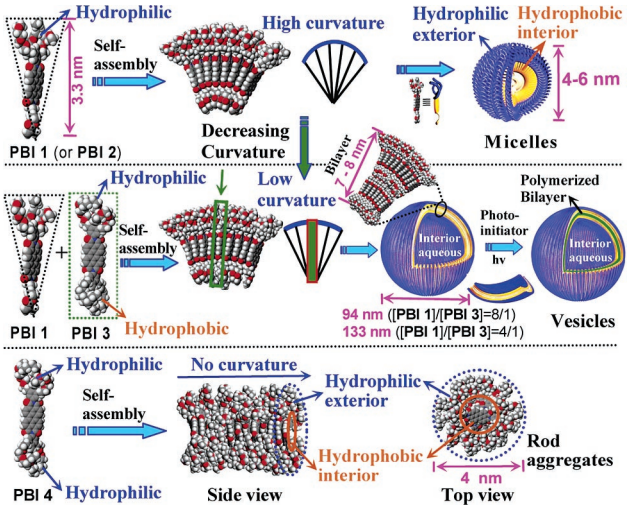

In summary, the aggregate morphologies of amphiphilic PBIs are dependent on their molecular shapes. The co-self-assembly of wedge-shaped PBI **1** and dumbbell-shaped PBI **3** generated hollow vesicles owing to the changes in spontaneous curvature. The bilayer structures of the vesicles could be stabilized by in situ photopolymerization. The morphology changes by co-self-assembly of different molecular architectures provide a guideline for the rational design of particular morphology such as vesicles.

Acknowledgment. We thank the Alexander von Humboldt Foundation (fellowship for Xin Zhang) and Theo Kaiser, Elisabeth Meyer-Natus, and Dr. Georg Krohne for their kind help.

Supporting Information Available: Synthetic details, spectroscopic characterization, UV−vis absorption, fluorescence and 2D NMR spectra of amphiphilic perylene bisimides, TEM images, and DLS data of aggregates. This material is available free of charge via the Internet at http://pubs.acs.org.

References

(1) Würthner, F. *Chem. Commun.* **2004**, 1564−1579.
(2) (a) Abdalla, M. A.; Bayer, J.; Rädler, J. O.; Müllen, K. *Angew. Chem., Int. Ed.* **2004**, *43*, 3967−3970. (b) Wang, W.; Wan, W.; Zhou, H. H.; Niu, S. Q.; Li, A. D. Q. *J. Am. Chem. Soc.* **2003**, *125*, 5248−5249.
(3) (a) Percec, V.; Dulcey, A. E.; Balagurusamy, V. S. K.; Miura, Y.; Smidrkal, J.; Peterca, M.; Nummelin, S.; Edlund, U.; Hudson, S. D.; Heiney, P. A.; Hu, D. A.; Magonov, S. N.; Vinogradov, S. A. *Nature* **2004**, *430*, 764−768. (b) Antonietti, M.; Förster, S. *Adv. Mater.* **2003**, *15*, 1323−1333. (c) Hill, J. P.; Jin, W. S.; Kosaka, A.; Fukushima, T.; Ichihara, H.; Shimomura, T.; Ito, K.; Hashizume, T.; Ishii, N.; Aida, T. *Science* **2004**, *304*, 1481−1483. (d) Hartgerink, J. D.; Beniash, E.; Stupp, S. I. *Science* **2001**, *294*, 1684−1688.
(4) (a) Uzun, O.; Sanyal, A.; Nakade, H.; Thibault, R. J.; Rotello, V. M. *J. Am. Chem. Soc.* **2004**, *126*, 14773−14777. (b) Arnt, L.; Tew, G. N. *J. Am. Chem. Soc.* **2002**, *124*, 7664−7665. (c) Percec, V.; Ahn, C. H.; Ungar, G.; Yeardley, D. J. P.; Möller, M.; Sheiko, S. S. *Nature* **1998**, *391*, 161−164.
(5) Müller, A.; O'Brien, D. F. *Chem. Rev.* **2002**, *102*, 727−757.
(6) (a) Yamamoto, T.; Fukushima, T.; Yamamoto, Y.; Kosaka, A.; Jin, W.; Ishii, N.; Aida, T. *J. Am. Chem. Soc.* **2006**, *128*, 14337−14340. (b) Zhang, X.; Li, Z. C.; Li, K. B.; Lin, S.; Du, F. S.; Li, F. M. *Prog. Polym. Sci.* **2006**, *31*, 893−948.
(7) Würthner, F.; Chen, Z.; Dehm, V.; Stepanenko, V. *Chem. Commun.* **2006**, 1188−1190.
(8) (a) Israelachvili, J. *Intermolecular and Surface Forces*, 2nd ed.; Academic Press: San Diego, CA, 1991. (b) $P_c = v/al$, where v is the effective molecular volume, a is the occupied area by hydrophilic chains, and l is optimal molecular length.
(9) (a) Bigay, J.; Gounon, P.; Robineau, S.; Antonny, B. *Nature* **2003**, *426*, 563−566. (b) Lippincott-Schwartz, J.; Liu, W. *Nature* **2003**, *426*, 507−508.

JA070994U